MICROAUVS II: CONTROL

Mathieu Kemp
Nekton Research, LLC
Durham, North Carolina
919-405-3993x275
fruitbat@nektonresearch.com

1. Introduction

MicroAUVs are of interest for a number of applications ranging from environmental monitoring to ordnance delivery. Because of their small size, MicroAUVs are inexpensive. This opens the door to applications where they are either disposable, or where they can be deployed in large numbers.

The development of MicroAUVs creates a number of problems, all of which size-related:

- the number of actuators and their efficiency decreases;
- computational power decreases;
- power storage decreases;
- number and accuracy sensors decrease.

As a consequence, MicroAUVs are generally underactuated.

In the companion paper, we discussed the successful development of two MicroAUVs [1]. MicroHunter™ [see Figure 1] uses a single, non-moving actuator, and Helical Klinotaxis, Nekton's proprietary guidance technology. Ranger™ uses a single vectored-thruster and more classical control methods. Although underactuated, these vehicles are each capable of controlling their depth and heading. In this article, we discuss the theoretical foundation of Helical Klinotaxis.

2. Theory of Helical Klinotaxis

MicroHunter (Figure 1) is a class of MicroAUVs developed under DARPA sponsorship to serve as platform for distributed underwater robotics system. MicroHunters travel helically. They use a guidance algorithm, Helical Klinotaxis[2], that permits orientation to a vector field using a single sensor-actuator pair.

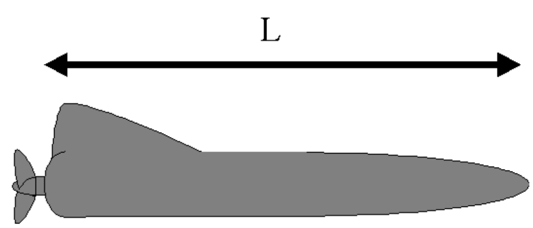

Figure 1. Schematics of the MicroHunter. The vehicle is composed of a hull, a fin, and a prop. The length of the vehicle is L.

Working HK has been demonstrated on two prototypes, the 15cm-long M3 and the 30cm-long M4 [1]. Tracking to a light source has been shown for both prototypes. Orientation to a compass heading at a given depth has been shown on the larger M4.

HK is based on the observation that a helically traveling object is able to change its heading by modulating propeller speed. To make this sensible, consider a vehicle that moves at constant speed along the hull axis with constant angular velocity along the hull and the lateral axis. This vehicle travels helically. The direction of net travel is parallel to the angular velocity vector.

Consider now an abrupt change of angular velocity. In response to the change, the vehicle changes heading. The new heading is determined by the direction where the angular velocity vector points *immediately after the change.* As will be discussed later, changing the propeller speed of MicroHunter changes the angular velocity of MicroHunter. Thus changing propeller speed changes the heading of the vehicle.

The change in heading is determined by the phase around the helix axis at which the vehicle was when the angular velocity changed. Changing propeller speed in open-loop fashion will in general produce random heading changes. HK is a method for appropriately coupling signal intensity to propeller speed so as to produce deliberate heading changes.

Existing theories of HK are kinematic [2-5]. Their applicability to MicroHunter is arguable because, the steady-state linear and angular velocities change proportionally in response to propeller speed changes. The prediction of the kinematic theory is that the heading should not change. The heading does change however, as has been observed on the actual vehicle. From this, we conclude that heading changes happen during the transient that follows a propeller speed change. Thus, a theory of MicroHunter control must be approached dynamically.

2.1. Equations of Motion

Because finite angular velocity is central to HK, a 6DOF formulation of the dynamics is used. We consider a MicroHunter of length L moving through a fluid. We define inertial orthonormal axes $\mathbf{e}_i$ and body axes $\mathbf{b}_i$ ($\mathbf{b}_1$=hull axis, $\mathbf{b}_2$=lateral axis, $\mathbf{b}_3$=fin axis). We define the body rotation matrix as $\mathbf{b}_i = R_{ij}\ \mathbf{e}_i$. We write the location of the vehicle's center of mass as $x_i\mathbf{e}_i$. We write the body-referenced linear and angular velocities as u_i and ω_i respectively. We write the effective mass matrix and moment of inertia of the vehicle as $[M_{ij}]$ and $[I_{ij}]$ respectively. We define the angular velocity dual $\Omega_{ij}=\omega_k\varepsilon_{kij}$. We write the hydrodynamic forces and moments as $\mathbf{F_u}$ and $\mathbf{F_\omega}$ respectively. We write the propeller thrust and torque as $T_i\mathbf{b}_i$ and $\tau_i\ \mathbf{b}_i$. We define S_i as the normalized vector pointing in the direction of maximum response of the sensor in the body frame. We define B_i as the normalized external field vector in the lab frame.

The equations of motion of MicroHunter are:

$$\frac{dx_i}{dt} = R_{ji}u_j \tag{1}$$

$$\frac{dR_{ij}}{dt} = \Omega_{ik}R_{kj}$$

$$\frac{du_i}{dt} = M^{-1}_{ik}\left[\boldsymbol{\omega} \wedge \mathbf{Mu} + \mathbf{F_u} + \mathbf{T}\right]_k$$

$$\frac{d\omega_i}{dt} = I^{-1}_{ik}\left[\boldsymbol{\omega} \wedge \mathbf{I}\boldsymbol{\omega} + \mathbf{F_\omega} + \boldsymbol{\tau}\right]_k$$

2.2. Control Algorithm

As discussed above, Helical Klinotaxis is a method for appropriately coupling signal intensity to propeller speed so as to produce deliberate heading changes. The method consists in coupling propeller output linearly to the sensor:

$$\mathbf{T} = \left[p_o + \gamma S^{+}RB\right]\mathbf{T_{max}} \tag{2}$$

$$\boldsymbol{\tau} = \left[p_o + \gamma S^{+}RB\right]\boldsymbol{\tau}_{\mathbf{max}}$$

where $\mathbf{T_{max}}$ and $\boldsymbol{\tau}_{\mathbf{max}}$ are the maximum prop trust and torque, p_o is the zero signal motor load, and γ is the gain.

2.3. Force Model

We make the assumptions that the vehicle is neutral, that the Reynolds number is high, that skin friction can be neglected, and that the hydrodynamic forces and moments are bilinear in u and ω. Then:

$$F_{ui} = A_{ijk} u_j u_k + B_{ijk} u_j \omega_k + C_{ijk} \omega_j \omega_k$$
$$F_{\omega i} = D_{ijk} u_j u_k + E_{ijk} u_j \omega_k + F_{ijk} \omega_j \omega_k \tag{3}$$

Equations 1-3 are general. They contain 126 hydrodynamic coefficients and 18 inertia terms. We find the inertia coefficients using the coefficients of an ellipsoid of revolution [5]. We find the force coefficients by system identification: the MicroHunter was mounted with three LEDs and its acceleration and deceleration profiles were captured using 3D tracking equipment. Linear and angular position, velocity, and acceleration were then use to construct the force model [Figure 2]. The model assumes that the only non-zero hydrodynamic coefficients are: A_{111}, A_{212}, A_{313}, B_{211}, D_{213}, D_{211}, D_{312}, E_{111}, and E_{311}, and that thrust and torque are directed along the 1-axis:

$$\mathbf{T}_{\mathbf{max}} = |\mathbf{T}_{\mathbf{max}}|[1 \quad 0 \quad 0] \tag{4}$$
$$\boldsymbol{\tau}_{\mathbf{max}} = |\boldsymbol{\tau}_{\mathbf{max}}|[1 \quad 0 \quad 0]$$

2.4. Linearization/Decoupling

Referring to Equations 1-3, we see that the force model is non-linear, and that the equations are coupled. We have found that extreme care must be taken in the selection of the linearization and decoupling procedure:

Linearization: linearization of the force model was performed around an operating point dictated by the steady state motor load. Using the result of the Appendix, the steady state operating point at p_{SS} (to be determined shortly) is

$$\mathbf{u}_{SS} = \sqrt{p_{SS}}\,\mathbf{u}(1)$$
$$\boldsymbol{\omega}_{SS} = \sqrt{p_{SS}}\,\boldsymbol{\omega}(1) \; . \tag{5}$$

Let us write

$$\mathbf{X} = \begin{bmatrix} \mathbf{u} \\ \boldsymbol{\omega} \end{bmatrix} = \begin{bmatrix} \mathbf{u}_{SS} \\ \boldsymbol{\omega}_{SS} \end{bmatrix} + \begin{bmatrix} \Delta\mathbf{u} \\ \Delta\boldsymbol{\omega} \end{bmatrix} = \mathbf{X}_{SS} + \boldsymbol{\Delta} \tag{6}$$

and

$$\begin{bmatrix} p\mathbf{T}_{\mathbf{max}} \\ p\boldsymbol{\tau}_{\mathbf{max}} \end{bmatrix} = p\boldsymbol{\Phi} = p_{SS}\boldsymbol{\Phi} + (p - p_{SS})\boldsymbol{\Phi} \; . \tag{7}$$

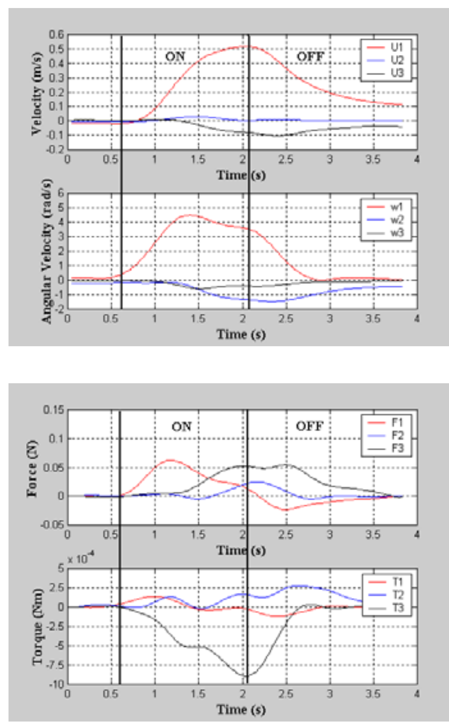

(4)

Figure 2. Transient response of the M3. The prop is initially off, then on for 1.5s, and finally off. Top: linear and angular velocity transients. Bottom: force and torque transients.

Expanding the force model around $\mathbf{X}_{SS}$, we write

$$\mathbf{G} = \begin{bmatrix} M^{-1}[\boldsymbol{\omega} \wedge \mathbf{Mu} + \mathbf{F}_{\mathbf{u}}] \\ I^{-1}[\boldsymbol{\omega} \wedge \mathbf{I}\boldsymbol{\omega} + \mathbf{F}_{\boldsymbol{\omega}}] \end{bmatrix} = \mathbf{G}_{SS} + J\boldsymbol{\Delta} \tag{8}$$

which leads to the linear equation

$$\frac{d\mathbf{\Delta}}{dt} = J\mathbf{\Delta} + (p - p_{SS})\mathbf{\Phi}. \quad (9)$$

We note that the jacobian scales with p as

$$J(p) = \sqrt{p}J(1). \quad (10)$$

Decoupling: motor load and vehicle orientation are coupled through the signal. In order to decouple them, we first define a signal variable:

$$\Sigma_i = R_{ij}B_j. \quad (11)$$

The signal at the sensor is $\mathbf{S}^+\Sigma$. At orientation, the steady-state angular velocity is parallel to the external field. We therefore write

$$\mathbf{\Sigma} = \frac{\boldsymbol{\omega}_{SS}}{|\boldsymbol{\omega}_{SS}|} + \boldsymbol{\sigma} \quad (12)$$

where $\boldsymbol{\sigma}$ is the correction from steady state. Since

$$p - p_{SS} = p_o + \gamma\mathbf{S}^+\mathbf{\Sigma} - p_{SS} = \gamma\mathbf{S}^+\boldsymbol{\sigma}, \quad (13)$$

we can write

$$\frac{d\mathbf{\Delta}}{dt} = J\mathbf{\Delta} + \gamma\mathbf{\Phi}\mathbf{S}^+\boldsymbol{\sigma}. \quad (14)$$

The differential equation obeyed by $\boldsymbol{\sigma}$ is:

$$\frac{d\boldsymbol{\sigma}}{dt} = \Omega_{SS}\boldsymbol{\sigma} - \frac{\Omega_{SS}}{|\boldsymbol{\omega}_{SS}|}\mathbf{\Delta\omega} + O(\boldsymbol{\sigma}\mathbf{\Delta\omega}). \quad (15)$$

Decoupling is achieved by dropping the second order term.

The linearization/decoupling procedure is only valid when the gain is small (linearization), and when the vehicle heading points near the direction of the external field (decoupling).

2.5. Results

Linearization/decoupling leads to a linear system of 9 equations:

$$\frac{d\mathbf{Z}}{dt} = \Gamma\mathbf{Z} \quad (16)$$

where

$$\mathbf{Z} = \begin{bmatrix} \mathbf{\Delta u} \\ \mathbf{\Delta\omega} \\ \boldsymbol{\sigma} \end{bmatrix}, \ \Gamma = \begin{bmatrix} [J] & \gamma\mathbf{\Phi}\mathbf{S}^+ \\ \begin{bmatrix} 0 & -\dfrac{\Omega_{SS}}{|\boldsymbol{\omega}_{SS}|} \end{bmatrix} & \Omega_{SS} \end{bmatrix}. \quad (17)$$

The dynamical matrix Γ has four components: J governs the free dynamics of u and ω; Ω_{SS} governs the free dynamics of the signal; the bottom left term couples the dynamics of the body to that of the signal; the upper right term couples the signal to the body. We note that the last contribution is proportional to the HK gain.

The dynamics of relaxation can be understood in terms of the poles of Γ. Figure 3 shows the trajectory followed by a well-tuned M3. In the absence of coupling, the six free dynamics poles have negative real parts. The three free signal poles are located at 0 and $\pm i|\omega_{SS}|$. When the coupling is turned on, the six free dynamics poles remain far to the left, the zero pole stays unchanged (antisymmetric nature of Ω_{SS}), and the other two poles develop a negative real component. (15)

The poles nearest the imaginary axis govern the rate of orientation of the vehicle. Let us define orientation as:

$$O = \frac{\boldsymbol{\omega}_{SS}^+\mathbf{\Sigma}}{|\boldsymbol{\omega}_{SS}|} = \cos(\theta) \quad (18)$$

where θ is the angle between the vehicle heading and the external field. Note the O≤1, 1 being perfect orientation. Using Equation 12:

$$1 - O = -\frac{\boldsymbol{\omega}_{SS}^+\boldsymbol{\sigma}}{|\boldsymbol{\omega}_{SS}|} = ae^{st} \quad (19)$$

which follows by restricting the expansion to the dominant pole. The exponential decrease of 1-O is shown in Figure 4.

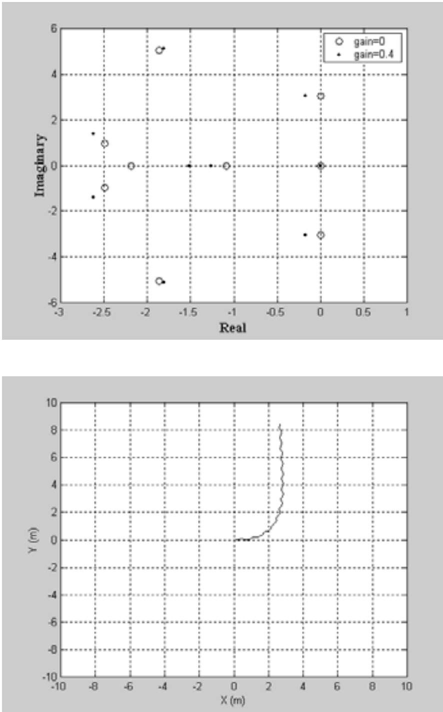

Figure 3. Pole placement of tuned M3 and resulting dynamics (30 seconds). Circles: zero gain poles. Dots: 0.4 gain poles.

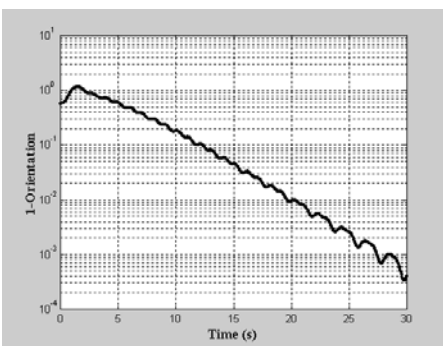

Figure 4. Time development of orientation. The error decreases exponentially fast.

2.6. Sensor Placement

The effect of sensor location is now addressed. As just discussed, the poles near the imaginary axis determine the dynamics of orientation. To determine these poles, we use Green's function techniques. First, we use partitioning to write the lower right Green's function component:

$$\left[\Omega_{SS} - \begin{bmatrix}0 & \dfrac{-\Omega_{SS}}{|\boldsymbol{\omega}_{SS}|}\end{bmatrix}[J-s]^{-1}\left[\gamma\boldsymbol{\Phi}\mathbf{S}^{+}\right] - s\right]G(s) = 1 \tag{20}$$

where s is the pole variable and G the lower right Green's function. Second, we use first order perturbation theory to find the pole nearest $i|\omega_{SS}|$:

$$\begin{aligned} s &= i|\boldsymbol{\omega}_{SS}| + i\gamma\left[\left[\mathbf{0} \quad \varphi^{+}\right][J-s]^{-1}\boldsymbol{\Phi}\right]\mathbf{S}^{+}\varphi \\ &= i|\boldsymbol{\omega}_{SS}| + i\gamma r e^{i\alpha}\mathbf{S}^{+}\varphi \end{aligned} \tag{21}$$

Here, φ is the eigenvector of Ω_{SS} associated with $i|\omega_{SS}|$. By antisymmetry of Ω_{SS}, φ is orthogonal to the steady state angular velocity ω_{SS}. Through a rotation of the plane orthogonal to ω_{SS}, it is possible to define new eigenvectors related to the old ones by a phase factor. In particular, we can pick new vectors $\chi=e^{-i\alpha}\varphi$ and write:

$$s = i|\boldsymbol{\omega}_{SS}| + i\gamma r\mathbf{S}^{+}\chi \tag{22}$$

This is explicit enough. The new pole is displaced from the old one by the rightmost term. Optimal sensor placement is achieved by making this term real and negative:

$$S_{optimal} = \sqrt{2}\,\mathrm{Im}(\chi) \tag{23}$$

All other sensor placements are suboptimal. Changing the placement of **S** moves the pole around $i|\omega_{SS}|$. Moving the pole around the optimal placement decreases the real part and eventually destroys the tracking abilities of HK.

An interesting consequence of Equation 21 is that the time for orientation scales as the square root of motor load. As noted previously, both the jacobian and the steady state angular velocity scale as the square root of p_{SS}. As Equation 21 reveals, the orientation rate is inversely proportional to J and ω_{SS}. The time for orientation is therefore proportional to the square root of motor load.

An additional consequence of is that reducing the steady state motor load decreases the turning radius. This follows because the turning radius is proportional to velocity and to orientation time; since both scale with the square root of p_{SS}, the turning radius increases linearly with p_{SS}.

Appendix. Dependence of Steady-State Velocities on Motor Load

Consider a motor load p. In steady state, the third and fourth members of Equation 2.1 read

$$\begin{aligned} p\mathbf{T}_{\mathbf{max}} &= -[\boldsymbol{\omega} \wedge \mathbf{Mu} + \mathbf{F}_{\mathbf{u}}] \\ p\boldsymbol{\tau}_{\mathbf{max}} &= -[\boldsymbol{\omega} \wedge \mathbf{I}\boldsymbol{\omega} + \mathbf{F}_{\boldsymbol{\omega}}] \end{aligned} \tag{A.1}$$

Let $\mathbf{u}(1)$ and $\omega(1)$ be the p=1 solution. Because the right hand side is quadratic in the variables, it follows that

$$\begin{aligned} \mathbf{u}(p) &= \sqrt{p}\,\mathbf{u}(1) \\ \boldsymbol{\omega}(p) &= \sqrt{p}\,\boldsymbol{\omega}(1) \end{aligned} \tag{A.2}$$

In consequence, regardless of the load p, the steady-state velocities always point in the same direction.

Acknowledgments

This study was funded by DARPA under contract DAAN02-98-C-4030.

References

[1]. Schulz, B., (2001). "MicroAUVs 1: Platform Design and Multi-Agent System Deployment", these proceedings.

[2]. Crenshaw, H.C., L. Edelstein-Keshet (1993). "Orientation by helical motion—II. Changing the direction of the axis of motion." *Bull. Math. Biol*. **55**, 213-230

[3]. Kemp, M., (2001). "Note on the Kinematics of Helical Klinotaxis", *Nekton Technical Report NR-P8*.

[4]. Brokaw, C.J., (1958). "Chemotaxis of bracken spermatozoids." Ph.D. thesis. Cambridge University.

[5]. Crenshaw, H.C., (1993). "Orientation by helical motion—III. Kinematics of the helical motion of organisms with up to six degrees of freedom." *Bull. Math. Biol*. **55**, 197-212.

[6]. Lamb, H. *Hydrodynamics*, Cambridge Mathematical Press.